

diffuse intensity at the ordered superlattice points of 100, 110, etc., is also confirmed.

The diffuse scattering data of Spruiell and Stansbury on Ni₄Mo is well reproduced by the theory by setting $V_2/V_1=0.300$. This ratio, while not predictable from the ordered structure, is consistent with it. In addition, for completeness, the recent results of Mozer, Keating, and Moss on CuNi are briefly summarized, where it is shown that the theory applies as well to clustering systems as it does to ordering ones.

Finally, the case for a long-range oscillatory interaction in β -brass is reexamined. We show that only at the $\frac{1}{2}\frac{1}{2}\frac{1}{2}$ position in reciprocal space will the effect of

an interaction beyond V_1 be remarkable. It is thus suggested that very careful neutron-scattering data be collected above T_c at that position in order to test for the presence of longer-range interactions.

We hope by these papers to have demonstrated the usefulness of an approximate theory in generating some interesting information on the pair interactions in a variety of binary alloys. As the techniques for incorporating longer-range interactions into the more exact theories are developed, these will in turn demand more exacting data on binary alloys. It is thus our further hope that a systematic collection of such data will be forthcoming.

Shock Compression of Argon and Xenon. IV. Conversion of Xenon to a Metal-Like State*

MARVIN ROSS

Lawrence Radiation Laboratory, University of California, Livermore, California 94550

(Received 25 January 1968)

Experiments have been reported in which liquid argon and xenon have been shock-compressed up to two to three times their initial densities. An inspection of the two sets of data indicates a surprisingly large compressibility in xenon at high temperatures and compression. The results of calculations for argon and xenon indicate that the energy gap between the filled valence band and empty conduction band in xenon is decreasing rapidly with increasing density. Using these results, a theoretical Hugoniot curve has been calculated that is in good agreement with experiment. On the basis of these results, we conclude that the highest pressure xenon points, which are at 500 kbar and 18 000°K, represent a metallic-like form of xenon that is similar to cesium. This state is one in which the conduction bands are partially filled as in a metal, and it has been reached by a combination of temperature and compression.

I. INTRODUCTION

IN recent years, a considerable amount of interest has centered on the subject of the conversion of insulators to metals.^{1,2} This paper will discuss the possibility of such a conversion occurring in a highly compressed inert gas system.

A classic example of an insulator is an inert gas solid. It has a filled valence band, and its lowest excited states are from 8 to 12 eV higher in energy. Following traditional thinking, to convert an inert gas into a metal it would be necessary to compress it until the energy gap between the valence and conduction bands became small or disappeared, resulting in a transition to a metallic state.

A transition to a metallic state from an insulator has never been observed in an inert-gas system, because the compressions necessary to close the gap between the filled and empty bands have never been attained. However, with the advent of explosive shock techniques, it

has become possible to compress the liquid inert gases up to two to three times their initial normal densities. Recent shock experiments in argon and xenon have been reported in the literature^{3,4} and have been discussed in the previous papers in this series.⁴⁻⁶

The present report will show that as a result of high temperatures and compressions, compressed xenon is converted to a metal-like state in which electrons from the filled $5p$ valence band have been promoted to an unfilled $5d$ -like conduction band, resulting in a material which is similar to cesium at very high pressures.

II. REVIEW OF EXPERIMENTS

Figure 1 shows the experimental Hugoniot for argon, and Fig. 2 the experimental xenon Hugoniot. In a previous paper,⁵ the theoretical curve A in Fig. 1 was determined by the Monte Carlo method of statistical mechanics, using the pairwise additive intermolecular

³ R. N. Keeler, M. van Thiel, and B. J. Alder, *Physica* **31**, 1437 (1965).

⁴ M. van Thiel and B. J. Alder, *J. Chem. Phys.* **44**, 1056 (1966).

⁵ M. Ross and B. J. Alder, *J. Chem. Phys.* **46**, 4203 (1967).

⁶ M. Ross and B. J. Alder, *J. Chem. Phys.* **47**, 4129 (1967).

* Work performed under the auspices of the U. S. Atomic Energy Commission.

¹ N. F. Mott, *Phil. Mag.* **6**, 287 (1961).

² H. G. Drickamer, *Solid State Phys.* **17**, 1 (1965).

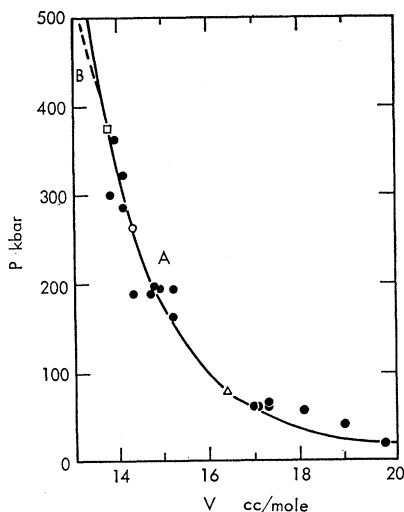


FIG. 1. Filled circles are experimental argon Hugoniot points. Curve A (solid line) is the theoretical argon Hugoniot with no electronic excitation. Curve B (dashed line) includes electronic excitation. Temperatures along the Hugoniot are signified by \square , 12 000°K; \circ , 8000°K; \triangle , 2000°K.

potential

$$\phi(r) = \epsilon \left\{ \left(\frac{6}{\alpha - 6} \right) \exp[\alpha(1 - r/r^*)] - \left(\frac{\alpha}{\alpha - 6} \right) \left(\frac{r^*}{r} \right)^6 \right\}, \quad (1)$$

where $r^* = 3.85 \text{ \AA}$, $\epsilon/k = 122^\circ\text{K}$, and $\alpha = 13.5$. The curve in Fig. 2 was calculated for xenon with $r^* = 4.47 \text{ \AA}$, $\epsilon/k = 235^\circ\text{K}$, and $\alpha = 13.5$, and was obtained by corresponding states scaling from argon using the ratios of

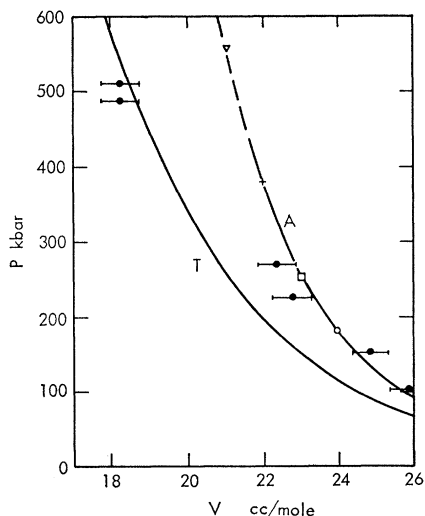


FIG. 2. Filled circles are experimental xenon Hugoniot points. Bars indicate experimental error. Curve A is the theoretical xenon Hugoniot that obeys corresponding states with the argon Hugoniot; T is the TFD curve. Temperatures along the Hugoniot curve are signified by ∇ , 30 000°K; +, 18 000°K; \square , 12 000°K; \circ , 8000°K.

the triple-point measurements. The solid part of this curve denotes the range of the argon experiments of Fig. 1 also scaled up to xenon by corresponding states. The over-all agreement of theory with experiment is very good in the case of argon, whereas agreement with the xenon measurements, though good at low pressures, becomes poor at high pressures. Since argon and xenon are inert gases with closed-shell configurations, one would expect to observe approximately corresponding behavior in their thermodynamic properties. While some deviations might be anticipated in the two Hugoniot as a result of the possible nonapplicability of corresponding states under these conditions, the large observed discrepancies between the two sets of experiments would not be expected. Qualitatively, it is possible to account for these differences by the following considerations. It is shown in Fig. 1 that the maximum temperature attained along curve A is about 1 eV in argon and would be 2 eV in xenon if it had obeyed corresponding states. The first excited state of atomic xenon is 8.4 eV as compared to 11.6 eV in argon. It is, therefore, to be expected that as a result of the high temperatures, xenon will undergo considerably more electronic excitation than argon, and its Hugoniot will be softer as a result of absorbing energy in internal degrees of freedom rather than as thermal pressure.

In a previous publication,⁶ the effect of electronic excitation was treated quantitatively by using the temperature-dependent, Thomas-Fermi-Dirac (TFD) model of the atom. The nuclear motion contributions to the thermodynamic properties were calculated using the Lennard-Jones-Devonshire (LJD) cell model.⁷ A severe limitation of the TFD theory is that, because it is based only on electrostatic theory and Fermi-Dirac statistics, it has no band structure or region of forbidden energy states, but instead allows electrons to be excited into a continuous series of energy levels immediately above the ground state. Consequently, the TFD model correctly predicts the average Hugoniot of argon and xenon, but fails to show some of the more subtle behavior, such as the effects of stripping off shells of electrons when the temperature becomes comparable to the gap in energy between the filled and empty bands. This is seen in Fig. 2 where the TFD curve for xenon, which was calculated in the previous publication,⁶ is shown by the dashed curve T. The pressure of curve T is too low at low pressures because the electrons are excited into the low-lying levels just above the valence band at relatively low temperatures, and there is no bending over at high temperatures as the result of the sudden onset of electronic excitation. Instead, one observes a gradual behavior as the Hugoniot goes from low to high temperatures, which is in good average agreement with xenon. This averaged-out type of agreement is a typical characteristic of the Thomas-Fermi theory. The TFD

⁷ J. O. Hirschfelder, C. F. Curtiss, and R. B. Bird, *Molecular Theory of Gases and Liquids* (John Wiley & Sons, Inc., New York, 1954).

curve is not shown for argon, but is in good agreement with the experiment. In order to overcome this defect of the TFD model, it is necessary to introduce into Hugoniot calculations energy levels which are discrete and, therefore, more realistic. For this purpose, the Wigner-Seitz model was used to calculate the energy levels of an electron moving in the crystal potential of the TFD compressed atom. These calculations were made over a large range of volumes, and are described in Sec. III. Section IV discusses the thermodynamics of a system of electrons with a band structure that is a function of volume. In Sec. V, thermodynamic equations derived in Sec. IV are combined with the energy levels calculated in Sec. III and are used to calculate Hugoniots for argon and xenon.

III. ELECTRONIC ENERGY LEVELS

In this section, the Wigner-Seitz model will be used to calculate discrete electronic energy levels for the TFD compressed atom as a function of volume, using the TFD crystal potential.

In the Wigner-Seitz⁸ method, the Schrödinger equation is solved in a spherical cell of atomic volume, with the boundary conditions on the wave function and its derivative as imposed by the Bloch condition. Solutions of the Schrödinger equation were obtained for only the points of highest symmetry in the Brillouin zone at $k=0$. For these states the boundary conditions on the one-electron radial wave function, $f(r)$, at the cell surface $r=R$ can be shown to be⁹

$$\begin{aligned} f'(R) &= 0, & l &= 0, 2, 4, \text{ even}, \\ f(R) &= 0, & l &= 1, 3, 5, \text{ odd}, \end{aligned}$$

where $f'(R)$ is the derivative of $f(r)$ at R and l is the angular momentum quantum number. The alternate solutions $f'(R)=0$, with l odd, and $f(R)=0$ with l even, are often taken to give estimates of the energy at the maximum k values in a band.¹⁰ These latter solutions do not enter into any of the quantitative considerations of this paper, but are useful in estimating the width in energy of the valence bands. The crystal potential of the electron used in solving the Schrödinger equation was determined from the TFD model of the solid calculated for the same atomic volume as used in the Wigner-Seitz calculations. As a result of both models using identical cells, it was possible to calculate a new potential energy and electron density for each density. The crystal potential was of the form

$$U(r) = V(r) - 6[(3/8\pi)\rho(r)]^{1/3},$$

where $V(r)$ is the Coulombic interaction of a test charge with the nucleus and all of the electrons as calculated by TFD and does not include the exchange as it is calcu-

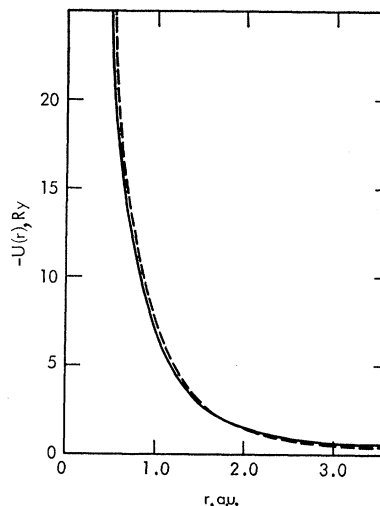


Fig. 3. Comparison of argon crystal potential due to Mattheiss (dashed curve) and that derived from TFD and used in present work (solid curve) at V of 22.6 cc/mole. r is in atomic units.

lated by TFD. Instead, the exchange was added separately. It is given by the last term which is the usual Hartree-Fock-Slater exchange term,¹¹ and $\rho(r)$ is the electron density calculated by TFD. The TFD calculations have been discussed previously. In addition, it has already been shown⁶ that $\rho(r)$ for atomic argon is in good agreement with $\rho(r)$ calculated by Herman and Skillman¹² using a self-consistent Hartree-Fock-Slater method. The TFD calculated $\rho(r)$ does not show the detailed shell structure, but does correctly predict the averaged behavior. Figure 3 shows the crystal potential used for argon at $r=22.6$ cc/mole (solid curve) compared to one used by Mattheiss¹³ (dashed curve) in an augmented-plane-wave (APW) band calculation. The results of the calculations are shown in Figs. 4 and 5,

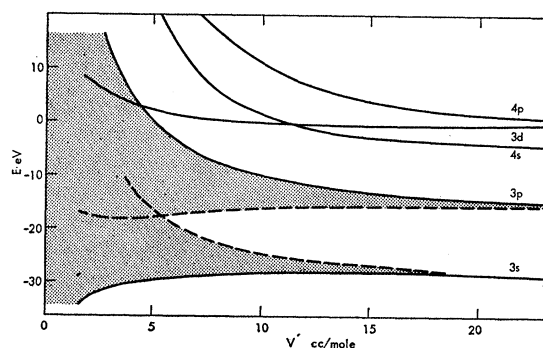


Fig. 4. Calculated energy levels of argon with atomic notations. Solid curves are solutions for $k=0$. Dashed curves show bandwidth based on the estimate of the energy at the maximum k value.

¹¹ J. C. Slater, *Quantum Theory of Atomic Structure* (McGraw-Hill Book Co., New York, 1960), Vol. 2.

¹² F. Herman and S. Skillman, *Atomic Structure Calculations* (Prentice-Hall, Inc., Englewood Cliffs, N. J., 1963).

¹³ L. F. Mattheiss, *Phys. Rev.* **133**, A1399 (1964).

⁸ E. Wigner and F. Seitz, *Phys. Rev.* **46**, 1002 (1934).

⁹ H. Brooks, *Nuovo Cimento Suppl.* **7**, 186 (1948).

¹⁰ J. C. Slater, *Phys. Rev.* **45**, 794 (1934).

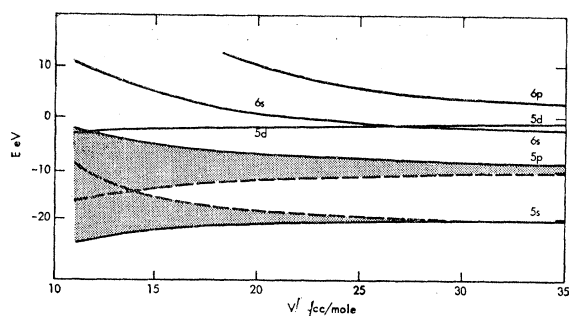


FIG. 5. Same as Fig. 4 but for xenon.

and are based on taking $V(r)=0$ at the cell boundary. In discussing the energy levels, atomic notations are retained. The calculations take no cognizance of crystal-field splitting and they assume a single s state, the p state to be threefold degenerate, and the d band to be fivefold degenerate, as in the free atom.

Before analyzing the results, it is worthwhile to digress slightly and discuss the electronic transition found in cesium so that the properties of xenon and cesium may be best interrelated. In 1947, Bridgman¹⁴ reported that cesium underwent a first-order phase transition without a change in crystal structure (electronic transition) at a molar volume of 35 cc/mole, twice normal density, and a pressure of 42.5 kbar at 25°C. The interpretation of this transition was first presented by Sternheimer¹⁵ on the basis of a Wigner-Seitz model. He showed that at normal density (70 cc/mole) the lowest conduction band was s -like and the next lowest d -like. Under compression the empty d -like bands decreased in energy relative to the partly filled s -like, crossing the Fermi surface near 35 cc/mole, thereby resulting in the observed transition by promoting s -like electrons into the d -like conduction bands.

In the calculations for xenon shown in Fig. 5, the $6s$ band is the lowest conduction band at normal density and lies 6.8 eV above the valence band. The bottom of the $6s$ and $5d$ bands cross at about 27 cc/mole. This is the transition which cesium undergoes when the uppermost filled $6s$ levels at the Fermi surface intercept the $5d$ band, and, therefore, the observed transition occurs at a somewhat larger volume (35 cc/mole) than that predicted by the simple crossing of the two bands. This has been discussed by Sternheimer, and our xenon energy levels are in agreement with his cesium calculations. The present calculations predict that the valence band will intersect the conduction band at about 11.7 cc/mole, and a pressure at 0°K of about 0.7 Mbar based on TFD calculations. In argon, the $4s$ band at $k=0$ is the excited state of the lowest energy and lies 9.9 eV above the top of the valence band which is the $3p$ ($k=0$) state. The calculations predict that the $3d$ and $4s$ levels

will cross at a volume of 11.5 cc/mole. This is then the approximate region of volume at which potassium would be expected to undergo an electronic transition similar to the one observed in cesium. This transition has never been observed in potassium because the necessary compression of four times the initial density has never been achieved. At 4.5 cc/mole the conduction and valence bands cross, and argon should become metallic. Unfortunately, compressions of argon to this density and a pressure at 0°K based on TFD calculations of about 4.4 Mbar are far beyond the capability of static techniques, and even well outside the range that can be reached by explosive techniques.

Baldini¹⁶ has measured the ultraviolet spectra of Ar, Kr, and Xe. For argon he reports an absorption band edge at 11.2 eV, a lowest energy peak at 12.0, and by use of the Wannier exciton theory, he estimates the conduction band to be at 14.3 eV. In xenon these respective values are 8.0, 8.4, and 9.26 eV. The lowest energy peaks in all three solids are in good agreement with the lowest excited state of the free atom. In other theoretical calculations using considerably more sophisticated methods, Knox and Bassani,¹⁷ using an orthogonalized-plane-wave (OPW) method, and Mattheiss,¹⁸ using an APW method predicted, respectively, that the lowest conduction bands will be the s -like Γ_1 and will lie 12.4 eV (Knox) and 13.3 eV (Mattheiss) above the valence band. Using a somewhat more elaborate form of the Wigner-Seitz model than used here, Gandel'man¹⁸ used a Thomas-Fermi potential to estimate when argon would turn metallic. This model predicts a normal density band gap of 6 eV, which is from a $3p$ to a $3d$ state in disagreement with the works cited above. He predicts metallization in argon to occur at about 7 cc/mole and 1.29 Mbar at 0°K. In work to be reported,¹⁹ APW calculations have been made for argon and xenon at high compressions and the results are consistent with those in Figs. 4 and 5.

In the next section the thermodynamic treatment of the electron system is based on a spherical wide-band approximation. Figures 4 and 5 will clearly show this to be a good approximation in the high-pressure, high-temperature region of the Hugoniot where significant amounts of electronic excitation will be shown to occur. The APW calculations are in qualitative agreement with the estimated Wigner-Seitz bandwidths.

The purpose of the calculations in this section is to interpret the properties of a highly compressed fluid at temperatures of 1 to 2 eV. Therefore it will be assumed that the energy levels for argon and xenon depend only on density and not on temperature or on any specific atomic order (this assumption is implicit in the Wigner-

¹⁶ G. Baldini, Phys. Rev. **128**, 1562 (1962).

¹⁷ R. S. Knox and F. Bassani, Phys. Rev. **124**, 652 (1961).

¹⁸ G. M. Gandel'man, Zh. Eksperim. i Teor. Fiz. **48**, 758 (1965) [English transl.: Soviet Phys.—JETP **21**, 501 (1965)].

¹⁹ M. Ross (to be published).

¹⁴ P. W. Bridgman, Phys. Rev. **72**, 533 (1947); Proc. Am. Acad. Arts Sci. **76**, 55 (1948).

¹⁵ R. Sternheimer, Phys. Rev. **78**, 235 (1950).

Seitz model), and thus may also be applied to these fluids.

The Wigner-Seitz calculations shown in Figs. 4 and 5 are calculations made with the simplest model of a solid and only at the highest symmetry points. Consequently, only very limited information can be obtained as to the shape of energy bands and their changes with volume. The proper calculations can only be made by using more sophisticated approaches, and the Wigner-Seitz calculations can in no way replace them. However, these energy levels do constitute a significant improvement over the TFD model of a continuous set of energy levels, and as compared to the more sophisticated band calculations involve a very small amount of computational effort. In addition, the experimental conditions of a fluid at high temperatures is hardly compatible with the usual band-theory assumptions. Consequently, the present approach should prove useful in equation-of-state calculations over wide density ranges where the effects of gaps in the energy levels must be considered.

IV. STATISTICAL THERMODYNAMICS OF NONINTERACTING ELECTRONS WITH FORBIDDEN ENERGY LEVELS

In this section we will consider the statistical thermodynamics of a system of noninteracting electrons in valence and conduction bands which are well represented by spherical energy surfaces and in which the band edges are a function of volume. For this system, let $E_c(V)$ and $E_v(V)$ be the conduction and valence band edges; then the energy levels in the two bands are given by

$$E_c(V, k) = E_c(V) + \hbar^2 k^2 / 2m_c^*, \quad (2a)$$

$$E_v(V, k) = E_v(V) - \hbar^2 k^2 / 2m_v^*. \quad (2b)$$

$N(E)$ is the number of states with energy between E and $E+dE$ and is given for the conduction bands by

$$N(E) = N[E_c(V, k)] = 4\pi(g_c/h^3)V(2m_c^*)^{3/2} \times [E - E_c(V)]^{1/2}, \quad E \geq E_c(V) \quad (3a)$$

and for the valence bands by

$$N(E) = N[E_v(V, k)] = 4\pi(g_v/h^3)V(2m_v^*)^{3/2} \times [E_v(V) - E]^{1/2}, \quad E \leq E_v(V). \quad (3b)$$

The forbidden range of energy levels is defined by

$$N(E) = 0, \quad \text{if } E_v(V) < E < E_c(V).$$

The symbols g_c and g_v are the orbital degeneracies of the bands, V is the molar volume, and m_c^* and m_v^* are the effective masses of the electrons in the respective bands.

The free energy for this system of electrons is

given by²⁰

$$A_e = N\mu - kT \int_{-\infty}^{\infty} \{\ln[1 + e^{(\mu-E)\beta}]\} N(E) dE, \quad (4)$$

where N is the total number of electrons and μ is the chemical potential. By direct differentiation of (4) it can be shown that the pressure P_e and energy E_e are given by

$$P_e(T, V) = P^*(T, V) + P^0(V), \\ P^*(T, V) = -[\partial \Delta E(V) / \partial V]_{T, N_c} N_c(T, V) + P_c(T, V, N_c) + P_H(T, V, N_c) \quad (5)$$

and

$$E_e(T, V) = E^*(T, V) + E^0(V), \\ E^*(T, V) = \Delta E(V) N_c(T, V) + E_c(T, V, N_c) + E_H(T, V, N_c), \quad (6)$$

where $\Delta E(V) = E_c(V) - E_v(V)$, which is the difference in the energy of the valence and conduction band edges.

The terms $P^0(V)$ and $E^0(V)$ are the pressure and energy of the filled valence band at 0°K; $N_c(T, V)$ is the total number of electrons in the conduction bands; and $P_c(T, V)$, $P_H(T, V)$, $E_c(T, V)$, $E_H(T, V)$ are the pressures and energies due to the electrons in the conduction bands and the holes in the valence bands. By the usual method as described by Fowler²¹ to determine the number of conducting electrons in a semiconductor, one can show that

$$N_c(T, V) = 2(g_v g_c)^{1/2} \left(\frac{2\pi kT}{h^2} \right)^{3/2} (m_c^*)^{3/4} (m_v^*)^{3/4} \times \exp\left[-\frac{\Delta E(V)}{2kT} \right] V, \quad (7)$$

and results from the Boltzmann limiting case of small concentrations of excited electrons. The terms $A_e(T, V)$, $P_e(T, V)$, and $E_e(T, V)$ refer only to electronic properties and do not include the contributions from the nuclear motion which will be included in the Hugoniot calculations.

In Sec. V, the statistical thermodynamic formalism developed here will be combined with the energy levels of the previous section in a direct calculation of the Hugoniot.

Before proceeding further, it will be instructive to discuss certain qualitative aspects of the physics involved by comparing the experimental Hugoniot with the theoretical energy-level curves of Figs. 4 and 5. The smallest volume achieved along the experimental argon Hugoniot is 13.8 cc/mole, and at this volume the energy gap is unchanged from its initial value and the temperature is still small in comparison. In addition, the transition is from a threefold-degenerate p state to a single

²⁰ E. C. Stoner, *Phil. Mag.* 28, 257 (1939).

²¹ R. H. Fowler, *Statistical Mechanics* (Cambridge University Press, New York, 1936).

4s conduction band. However, in xenon in the volume range of 18 to 22 cc/mole where the Hugoniot is bending over, the 5d level has dropped below the 6s so that the lowest transition is to a fivefold-degenerate *d* state, and the energy gap is decreasing rapidly with decreasing volume. This will lead to enhancement in the electronic excitation, but in addition the $(\partial\Delta E/\partial V)_{T,N_e}$ term in (5) will contribute a negative term to the total electron pressure. As a result, one can anticipate that the resulting xenon Hugoniot will be significantly affected by the shape of the band, while argon will not.

V. HUGONIOT CALCULATIONS

The shock Hugoniot curve is obtained as a solution of the equation

$$E(T,V) - E(T_0,V_0) = \frac{1}{2}[P(T,V) + P(T_0,V_0)](V_0 - V). \quad (8)$$

The subscript 0 refers to the initial conditions which were $V_0 = 28.46$ cc/mole, $T_0 = 86^\circ\text{K}$ for argon, and $V_0 = 44.6$ cc/mole, $T_0 = 165^\circ\text{K}$ for xenon. Both substances are initially in the liquid in corresponding states with one another at $P(T_0,V_0) \approx 1$ bar.

Using (6) and adding to it the contribution to the energy from nuclear motion $E(T,V)_n$,

$$E(T,V) = E^*(T,V) + E^0(V) + E(T,V)_n.$$

We may then write

$$E(T,V) - E(T_0,V_0) = [E^*(T,V) - E^*(T_0,V_0)] + [E^0(V) - E^0(V_0)] + [E(T,V) - E(T_0,V_0)]_n. \quad (9)$$

The first term on the right-hand side of (9) is the change in energy due to electronic excitations and is, therefore, equal to $E^*(T,V)$, since the system is in its electronic ground state at T_0 and V_0 . The next term represents the change in electronic energy at 0°K due to compression and is therefore equal to the change in lattice energy on compression at 0°K . The last term is the change in thermal energy due to nuclear motion. Consequently, these two terms are simply the change in total energy on compressing and heating the system in its electronic ground state from (T_0,V_0) to (T,V) . This has been calculated by using the LJD cell model.⁷ Like the TFD and Wigner-Seitz models, the LJD cell model uses a spherical cell whose volume is that of the atomic volume. The LJD is a one-particle model and the atom moves in a potential field obtained by summing the pair potential over all its stationary neighbors and then taking its spherical average. The atom is taken to be in its electronic ground state. The energy of the system of N atoms in the LJD model is

$$E(T,V)_{\text{LJD}} = \frac{1}{2}NE(V) + \left[\frac{3}{2}NkT + NkT^2 \left(\frac{\partial \ln Q_1}{\partial T} \right)_V \right] \\ = U(V) + E(T,V)_{\text{thermal}},$$

where Q_1 , the one-particle partition function, is

$$Q_1 = \int_{\Delta} \exp\{-[E(r) - E(V)]/kT\} dv.$$

The integration is taken over the volume of the cell and $E(r)$ is the sphericalized potential field calculated using the pair potential of (1). r is the distance of the atom from the center of the cell. $\frac{1}{2}NE(V)$ is the lattice energy and represents the energy of the system at volume V when all atoms are located at their respective lattice sites and the term in brackets is the thermal energy of the system.

Then the change in electronic energy or lattice energy on compression at 0°K is

$$(E^0(V) - E^0(V_0)) = U(V) - U(V_0)$$

and

$$(E(T,V) - E(T_0,V_0))_n = (E(T,V) - E(T_0,V_0))_{\text{thermal}}.$$

We may then write (9) as

$$E(T,V) - E(T_0,V_0) = E^*(T,V) + E(T,V)_{\text{LJD}} - E(T_0,V_0)_{\text{LJD}}, \quad (10)$$

where

$$[E^0(V) - E^0(V_0)] + [E(T,V) - E(T_0,V_0)]_n \\ = E(T,V)_{\text{LJD}} - E(T_0,V_0)_{\text{LJD}}.$$

Adding the contribution to the pressure due to nuclear motion $P(T,V)_n$ to (5) gives us

$$P(T,V) = P^*(T,V) + P^0(V) + P(T,V)_n.$$

In the LJD model the pressure of the solid may be written as

$$P(T,V)_{\text{LJD}} = P(V) + P(T,V)_{\text{thermal}}.$$

The term $P(V)$ is the pressure of the lattice at 0°K and $P(T,V)_{\text{thermal}}$ is the thermal contribution to the pressure. Since $P^0(V)$ is the pressure of the solid at 0°K , then

$$P(T,V) = P^*(T,V) + P(T,V)_{\text{LJD}}.$$

In a previous publication⁵ it was shown by comparison to exact Monte Carlo calculations that for the potential (1) the cell model predicts a Hugoniot in good agreement with the Monte Carlo calculations and is, therefore, a reliable method of calculating the Hugoniot and thermal properties. Using (1), (10), and (11) in (8), Hugoniot calculations were made and the results are shown in Fig. 6. The Hugoniot curves were calculated from the Wigner-Seitz results of Figs. 4 and 5 and by adjusting the energy of the 3*p* and 5*p* valence states so that the transitions to the lowest excited states would agree with the conduction band gap as determined from the optical spectra using exciton theory. It was also assumed that m_e^* and m_v^* were equal to the electron mass m_e . In all of the calculations the electron densities were small enough and temperatures suffi-

ciently high such that the conduction electrons and holes could be treated as weakly degenerate gas. The calculations for argon in Fig. 1 (dashed curve B) show that the inclusion of electronic effects has negligible influence on its Hugoniot. However, the calculations for xenon, curve B, Fig. 6, show large electronic effects, and the results are in good agreement with experiment (± 0.5 cc/mole). If no adjustment had been made in the band gap and the calculated energy levels had been used then the predicted Hugoniot would have been in agreement with the lower part of the highest pressure points rather than with the upper part. Also shown in Fig. 6 is a Hugoniot curve C for which the term $(\partial\Delta E/\partial V)_{T,N_e}$ in $P^*(T,V)$ was neglected, but otherwise, the same calculation was carried out as in curve B. Curve C, while an improvement over curve A which includes only intermolecular forces and neglects any electronic excitations, still fails to predict the experimental result. The significance of this point will be expanded upon in the discussion. The results of the calculated xenon Hugoniot of curve B are shown in Table I. The $\Delta E(V)$ listed is the adjusted band gap. The value $N_e(E)$ near the highest experimental point is only 0.15 electron/mole in all five bands, justifying the use of Boltzmann statistics.

All the Hugoniot calculations were made using the same intermolecular force law (1), thereby assuming that these forces do not change significantly as a result of electronic excitation. This is probably a good approximation for small excitations, but is difficult to assess for the conditions of the experiment. Rather than become involved in arbitrary adjustment, these forces have been kept as unchanged.

VI. DISCUSSIONS

It is clear from Table I that the bending over of the xenon Hugoniot is coincident with the onset of significant amounts of electronic excitation. As discussed previously, this excitation decreases the amount of energy going into thermal pressure and results in a softer Hugoniot. However, a comparison of curves B and C shows that this effect alone is insufficient to account for the experimental results. It is also necessary to include the effect on the pressure of the decrease of the energy gap with compression, $\partial\Delta E/\partial V$. At the top of the valence band, $-\partial E_v(V)/\partial V$ is large and positive,

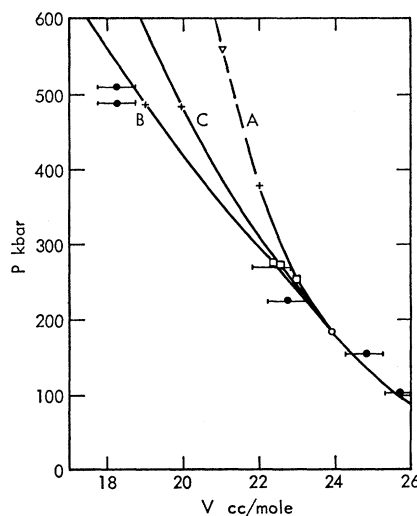


FIG. 6. Filled circles are experimental xenon Hugoniot points. Bars indicate experimental error. *A* is the theoretical xenon Hugoniot that obeys corresponding states with the argon Hugoniot, and *B* is the theoretical Hugoniot using the band results. *C* excludes effects of $-\partial\Delta E/\partial V$ on pressure. Temperatures along the Hugoniot curve are signified by ∇ , 30 000°K; +, 18 000°K; \square , 12 000°K; \circ , 8000°K.

while in the $5d$ band this derivative is negative. The result is a large negative contribution to the total pressure when an electron at the top of the valence band is excited into the $5d$ band. This decrease in the pressure amounts to 15% of the total pressure at 18.3 cc/mole. However, because of the thermal pressure of the free electrons, the total decrease only amounts to 9%.

The large value of $\partial E_v(V)/\partial V$ or broadening of the $5p$ band under pressure is a manifestation of the large repulsive forces between xenon atoms at small interatomic separations. Consequently, excitation of electrons into the $5d$ state, whose energy is decreasing with compression, has the effect of removing some of this repulsion, thereby lowering the pressure. This decrease in repulsion may be thought of as a decrease in the effective core size of the atoms or of a softening in the effective intermolecular force. For example one could have, in a purely phenomenological manner, interpreted the xenon Hugoniot in terms of a softening in the repulsive intermolecular force rather than in terms of electronic effects.

TABLE I. Summary of results.

T (°K)	V (cc/mole)	$\Delta E(V)$ (eV)	N_e (moles)	P (kbar)	$-(\partial\Delta E/\partial V)N_e$ (kbar)	P^* (kbar)	E (kcal/mole)	$(\Delta E)N_e$ (kcal/mole)	E^* (kcal/mole)
4000	25.70	9.23	$\sim 10^{-7}$	98.8	0	0	20.13	0	0
8000	23.88	8.89	0.008	182	-0.2	-0.1	42.9	0.2	0.2
12 000	22.40	8.53	0.015	271	-3.9	-2.5	69.6	2.9	4.0
16 000	20.30	7.86	0.074	396	-26	-16	113	13	20
18 000	19.00	7.34	0.134	484	-56	-35	146	23	37
18 500	18.66	7.19	0.153	509	-67	-41	156	25	43
19 000	18.31	7.03	0.174	536	-79	-49	166	28	48
20 000	17.62	6.69	0.222	594	-111	-68	189	34	61

In contrast to the results of the TFD theory, curve B predicts the correct shape of the Hugoniot because it includes a gap in the energy levels, and thereby predicts negligible excitation at low temperatures and a rapid onset of electronic excitation at the higher temperatures and compressions. Consequently, the present treatment is a more realistic approach to the calculation of insulator or semiconductor Hugoniots than could be obtained from TFD theory. At the highest pressures, curve B and the TFD curve are crossing. Since the TFD curve predicts averaged effects, it would be expected to crisscross an exact calculation a number of times as the pressure and temperature ionize more electron shells. Eventually, at very large compressions, the TFD will become exact.

One must conclude from these results that the highest-pressure xenon Hugoniot points represent a form of the material significantly different from that of the usual loosely bound inert-gas insulator. This state is one in which the $5d$ conduction bands are partially filled as in a metal and has been reached by the combination of temperature and compression. By compression alone at normal temperatures, the system would have to be compressed by a factor of about 5.5 from the initial conditions, before electrons could be promoted into the conduction band. However, because of the high temperatures achieved by the shock process, significant numbers of electrons can be excited into conduction bands so as to enable the electron promotion to take place at a significantly smaller compression.

The transitions in cesium and the bending of the xenon Hugoniot both occur as a result of the same qualitative change in their band structure, which is the decrease in energy under compression of the d -like conduction levels of the two materials. In cesium at 35 cc/mole, these levels fall below the Fermi surface promoting electrons into them, and the sharp increase in the number of available states of decreasing energy leads to the observed first-order phase transition. Under continued compression, as in shocked xenon, the d -like states become the lowest in the conduction band. These states continue to lower their energy with compression, resulting in a decrease in the energy gap above the valence band. This decreasing band gap along with the high temperatures generated in the shock experiments promote enough electrons into the d -like conduction band to convert xenon into a metal-like material, which is similar to cesium.

The question naturally arises as to whether this type

of electronic effect under shocked conditions may have occurred or can occur in other materials. The alkali halides are insulators with closed-shell atoms like the inert gases, and Kormer *et al.*²² have shock-compressed some of these to pressures of several megabars. One of the alkali halides studied, KCl, appeared to undergo a transition at a compression of 2.5 times its normal density, and a pressure of about 1.5 Mbar. Their data suggest the possibility of this transition being of first or second order; however, the experimental scatter is much too large to be definitive. These workers have observed transitions similar to KCl in KBr, NaCl, LiF, and possibly in CsI, but the data for the latter are somewhat incomplete. KCl has an initial molar volume of 37.6 cc/mole. If we assume each atom occupies an equal volume then the "atomic" volume per atom will be 18.8 cc/mole. When compressed 2.5-fold, this "atomic" volume will be 7.5 cc/mole. Since KCl is isoelectronic with argon, we may expect that the two materials will have qualitatively the same band structure. At normal densities, the conduction band gap in KCl is 7.5 eV so that if the $3p$ levels in Fig. 4 are adjusted to agree with experiment, then at the "atomic" volume of 7.5 cc the band gap is 4.9 eV to the $3d$ state and the band gap is closing rapidly. Since temperatures in this pressure range are of the order of 2 eV, then $\Delta E/2kT \sim 1.2$, and using (7) this leads to a predicted conduction-electron concentration of approximately 0.25 electron per atom or one conduction per two KCl molecules. Considering that the band gap is rapidly closing at these densities, it is even possible that the gap closing has been experimentally achieved. Consequently, one might expect some anomaly in the shock Hugoniot curve at this density and it would appear Kormer *et al.* may have shocked some of the alkali halides into a metal-like state. This argument is, of course, contingent on the assumption that the band structure of an alkali halide under large compression is qualitatively like its isoelectronic inert gas.

ACKNOWLEDGMENTS

We wish to acknowledge many valuable conversations with Dr. Berni J. Alder, and to thank Dr. Frank Herman and Dr. Edwin B. Royce for reading the manuscript.

²² S. B. Kormer *et al.*, Zh. Eksperim. i Teor. Fiz. 47, 1202 (1964) [English transl.: Soviet Phys.—JETP 20, 811 (1965)].